Forward Electron Production in Antimatter-Solid Collisions

Joachim Burgdörfer, Jianyi Wang, and Jörg Müller
Department of Physics, University of Tennessee, Knoxville, Tennessee 37996-1200, and Oak Ridge National Laboratory, Oak Ridge, Tennessee 37831-6377
(Received 28 October 1988)

We investigate the forward electron emission induced by fast antiprotons transmitted through thin carbon foils. The capture of electrons into wake-riding states is calculated in the second Born approximation. The transport through the foil is analyzed within the framework of classical stochastic dynamics. We find evidence that the usual cusp-shaped peak for positively charged ions is replaced by a broad peak due to emission of wave-riding electrons.

PACS numbers: 34.50.Fa, 05.40.+j, 79.20.Nc

Recent progress in the development of beams of antiparticles (positrons and antiprotons) with intensities sufficient for collision experiments affords the opportunity to study the behavior of atomic collision processes under charge conjugation of the impinging projectile in both the gas phase and condensed matter. The study of the dependence on the sign of the projectile potential is of significance from the viewpoint of a perturbational treatment of the collision since even and odd orders of the Born series have opposite parity under charge conjugation. This fact allows one to delineate the relative importance of higher-order terms of the series. The experimental[1] and theoretical[2] study of the total cross section for double ionization of He is an interesting case in point. Drastic changes under charge conjugation have also been found[3] in the differential single-ionization cross section of He under single-collision conditions.

Recently, the experimental study of antiproton transmission through carbon foils using the Low Energy Antiproton Ring facility at CERN has been proposed.[4] The purpose is to study the behavior of the stopping power and ionization under charge conjugation of the projectile (Barkas effect[5]), maintaining otherwise identical conditions of mass and velocity. Projectile energies in the first experiments presently underway are of the order of 1 MeV (corresponding to a beam velocity of $v_p \cong 6$ a.u.).

In the following we present the first investigation of the forward ionization spectrum induced by antiprotons transmitted through carbon foils. We will focus primarily on charge-conjugation effects for fast electrons with velocities $v_e \gtrsim v_p$ neglecting effects on slow "secondary" electrons. Our primary goal is to explore the possible existence of a peak of "wake-riding" electrons which was predicted some time ago[6] but has not yet been unambiguously observed. Two important features to be discussed in detail below make their observation in the forward-electron spectrum for antiprotons more likely than in the spectrum for positively charged ions: (a) The well-known cusplike enhancement in the forward spectrum of positively charged particles[7] is absent, thereby facilitating the observation of wake-riding electrons which appear in the same region of the spectrum, and (b) the wake-riding states are localized a factor of ~ 3 closer to an antiproton than to a proton of the same speed. Electron capture probabilities into wake-riding states are therefore dramatically enhanced.

Ejection of target electrons with large speeds $v_e \gg 1$ requires hard collisions at small impact parameters. Such processes will closely resemble ion-atom collisions since collective and condensed-matter effects are not important on this energy (or length) scale. For single collisions, the forward spectrum possesses two well-known features[8]: the binary-encounter peak at $v_e \simeq 2v_p$ which represents "classical" head-on Coulomb scattering and the "cusp" peak at $\mathbf{v}_e \simeq \mathbf{v}_p$ due to either electron capture to the continuum (ECC) or electron loss to the continuum (ELC).[7] While the binary-encounter process should be invariant under charge conjugation $Z_p \rightarrow -Z_p$ since classical Coulomb scattering does not depend on the sign of Z_p in the nuclear charge, the cusp peak depends sensitively on the sign of the final-state interaction factor

$$N(v) = \exp\left(\frac{Z_p \pi}{v}\right)\left|\Gamma\left(1 + i\frac{Z_p}{v}\right)\right|^2, \tag{1}$$

where $\mathbf{v} = \mathbf{v}_e - \mathbf{v}_p$ is the velocity vector in the rest frame of the projectile. An attractive final-state interaction between the electron and the ion ($Z_p > 0$) leads to a cusplike enhancement $\sim 2\pi Z_p / v$ of the cross section near $\mathbf{v}_e \approx \mathbf{v}_p$, while for $Z_p < 0$ a pronounced dip ("anticusp"[9]) $\sim (2\pi |Z_p|/v)\exp(-2\pi |Z_p|/v)$ occurs. The repulsive final-state interaction strongly inhibits forward scattering with small relative velocities v, thereby "burning" a hole into the forward spectrum and suppressing ECC. Clearly, ELC cannot occur because an antiproton ($\bar{p}$) ion does not support bound states. Even though an anticusp has not yet been experimentally observed, the behavior of the forward spectrum for ion-atom collisions seems to be well understood.

A qualitatively new situation occurs in a dense solid-state target. The interaction potentials are modified by collective effects in the dense medium and the post-foil spectral distribution is a result of a complex multiple-scattering process. Both dynamical screening by the medium and the transport properties of electrons in the field of the projectile depend on the sign of the projectile charge. The key point is that those solid-state effects,

© 1989 The American Physical Society

often overshadowed by the cusp for positive ions, can become visible for antiprotons because of the effective suppression of forward scattering.

The dielectric response of the medium to a swift ion induces collective charge-density fluctuations which result in an oscillatory polarization potential trailing the ion ("wake").[10] The wake supports bound states near the potential minima. Capture into this potential well and subsequent release into continuum states with velocities $\mathbf{v}_e \approx \mathbf{v}_p$ upon exit from the medium has been previously proposed as a mechanism for convoy electron production by positive ions.[6] Measurement of the Z_p and v_p dependence of this cusp shape were, however, at variance with this conjecture.[7]

The transition amplitude for electron capture into wake-riding states is given in second-order Born (B2) approximation by

$$t_{i,f} = \langle \phi_{\text{wake}} | V_p + V_t G_0 V_p | \phi_i \rangle , \quad (2)$$

where G_0 is the free-particle Green's function and $V_{p,t}$ are the (effective) interaction potentials of the projectile and target. At high speeds, capture from the carbon K shell dominates (i.e., $\phi_i = \phi_{1s}$). Accordingly, V_t can be taken as the bare Coulomb potential of the carbon nucleus with an effective value $Z_t = 5.7$, where we have taken into account screening effects by the passive $1s$ electron. The projectile potential V_p contains both the bare Coulomb potential and the dynamical screening potential. However, since capture requires a large momentum transfer in a hard collision and the dynamical screening potential is "soft," only the Coulomb part is important. For the ground state in the wake potential, $\phi^{(0)}_{\text{wake}}$, a harmonic-oscillator-type wave function, centered about the first wake minimum, was previously used. Detailed numerical investigations[11] of the wave functions for excited states show, however, that the harmonic-oscillator approximation becomes inadequate, in particular, for excited states $\phi^{(n)}_{\text{wake}}$ in the wake. Since the capture cross section depends sensitively on the tail of the wave function near the projectile, the contributions to the capture cross section from excited states with larger radii cannot be neglected. The evaluation of the capture cross section σ_c using Eq. (2) and standard techniques[12] reveals the remarkable result that the first-order Born term (B1) is negligibly small compared to the second-order Born term. This is a simple consequence of the fact that in the B1 approximation, capture is mediated by high-momentum components of the initial- and final-state wave functions. However, the "soft" wake potential exponentially suppresses high-momentum components in ϕ_{wake} leading to an exceedingly small cross section.[13] The dominant contribution is therefore provided by the second-order Born term in Eq. (2) which closely resembles the well-known Thomas double-scattering mechanism[14] for ion-atom collisions. Here an electron is first scattered off the projectile by $\approx 60°$, followed by a second deflection at the target by about 60°, such that the electron finally propagates in approximately the forward direction at zero speed relative to the projectile. The fact that V_p is repulsive for antiprotons rather than attractive for positively charged ions is immaterial since pure Coulomb scattering is invariant under charge conjugation ($Z_p \rightarrow -Z_p$) and resulting differences in the phase factor in the B2 term cancel because the B1 term is negligible. The crucial sign dependence on the sign of the projectile charge stems from the fact that the center of gravity of the final state ϕ_{wake} is displaced relative to the coordinate of the potential V_p by a distance $d \simeq (2 + \text{sgn}Z_p)\lambda/4$, where $\lambda = 2\pi v_p/\omega_p$ is the wavelength of the wake oscillations and ω_p is the plasma frequency. Charge conjugation leads to a phase shift of π in the dielectric polarization potential such that the first binding well for electrons in the wake behind the projectile is a factor 3 closer to an antiproton than to a proton. This proximity is crucial in determining the size of the cross section because the capture requires, in addition to velocity matching, a nonvanishing spatial overlap between the wave packet of the scattered electron and the final state ϕ_{wake}.

The velocity dependence of σ_c for capture into the ground state of the wake in the harmonic-oscillator approximation of the wake near an antiproton is displayed in Fig. 1. At $v_p \simeq 6$ a.u. the cross section per carbon atom is of the order of $\sigma_c \approx 10^{-22}$ cm^2. In the calculation of the forward spectrum at $v_p = 6$ a.u., we have included contributions from the first two excited wake states (one of which is a resonance) using numerically calculated wake-riding states[11] in separable form which increase the cross section by a factor of 3. Considering the high solid target density and the fact that additional

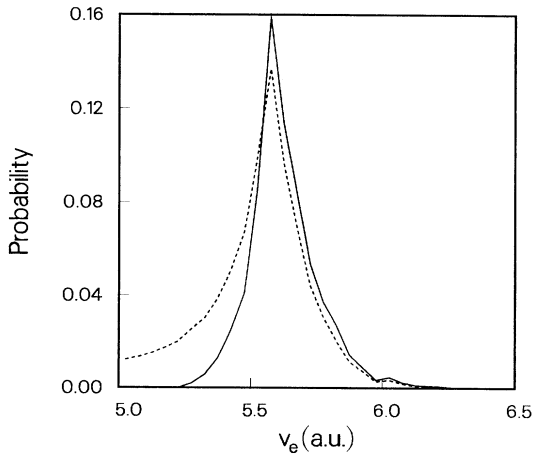

FIG. 1. Cross sections as a function of the velocity v_p of $\bar{p}$ used as input for the classical transport simulation. ——, cross section for capture of a carbon K-shell electron into the ground state (harmonic-oscillator approximation) of the first binding well of the wake of $\bar{p}$; ---, cross section for electron ejection with laboratory velocities $v_e > v_p$ in a binary collision with $\bar{p}$ in first Born approximation.

contributions from outer target shells have been neglected, the experimental observation should be within reach. For protons, on the other hand, the cross section is several orders of magnitude ($\gtrsim 6$) smaller in the velocity range under consideration because of the rapid decay of spatial overlap. This very likely accounts for the fact that wake-riding electrons have not yet been found.[7]

The wake-riding electrons, as well as electrons generated in binary-encounter events, suffer multiple scattering before exiting from the foil. The determination of the observable emission spectrum requires the study of the electron transport in the presence of the field of the nearby projectile. We employ a microscopic Langevin equation,

$$\frac{d}{dt}\mathbf{v} = -\nabla V_p + \mathbf{F}(t)\,, \tag{3}$$

describing classical trajectories of an electron under the influence of the field of the projectile (V_p) including the wake field. The electrons are subject to random forces $\mathbf{F}(t)$ representing stochastic collisions inside the solid. Details will be given elsewhere.[15] The complete solution of the transport problem is given by a Monte Carlo sampling of an ensemble of initial conditions for the phase-space coordinates which are propagated according to Eq. (3).

The phase-space distribution of initial conditions consists of both binary-encounter (BE) electrons and wake-bound electrons. For the simulation of the initial velocity distribution of BE electrons, a first-order Born approximation for ionization has been employed. Only energetic electrons with $v_e \gtrsim 0.8 v_p$ have been included in the transport calculation. The integrated BE cross section σ_{BE} for energetic electrons $v_e \gtrsim v_p$ (Fig. 1) is several orders of magnitude larger than σ_c. In order to improve the statistics we have calculated the stochastic evolution of wake-bound electrons separately and added their distribution function, weighted by their relative cross section, to the binary distribution. The initial classical distribution of the wake-bound electrons is determined by the spatial probability density distribution $|\phi_{\mathrm{wake}}(\mathbf{r})|^2$ restricted to the classically allowed region and by a uniform distribution over all negative energies larger than the value of the wake minimum.

In order to relate the dynamical evolution in the bulk to the post-foil experimental observation, modifications due to the penetration of the exit surface must be taken into account. The sudden breakdown of the dynamical screening near the projectile at the surface leads to a redistribution of the final-state population. This has particularly dramatic effects for wake-riding electrons that are in the close proximity of a repulsive Coulomb field of the antiproton. Figure 2 shows the velocity distribution of wave electrons scattered at the antiproton near the exit surface. The initial distribution prior to the break down of screening was an isotropic velocity distribution of the classical wake-bound states centered about the projectile ($v_z = v_p = 6$ a.u.). The effect of defocusing is clearly visible.

The resulting forward electron emission spectrum into a cone with half-angle Θ_0 is determined by the propagated phase-space distribution averaged over all contributing escape depths. This layer average determines the steady-state electron distribution. The resulting distribution at electron velocities near the projectile velocity ($5 \leq v_e \leq 7$) is shown in Fig. 3 for $v_p = 6$ a.u. and cone half-angles $\Theta_0 = 5°$ and 2.5°.

In the absence of a usual cusp, three features are clearly visible: a steep rise at the upper end of the spectrum which signifies the remnants of the anticusp valley in the single-collision spectrum, a background due to multiply scattered binary electrons inside the valley, and a broad peak due to emission of wake-riding electrons near $v_e \gtrsim 5.6$ on top of it. Since the wake-riding electrons give rise to a well-localized peak while the binary spectrum shows locally little angular dependence, the peak due to wake-riding electrons should become the dominant feature for sufficiently small Θ_0 (Fig. 3). The

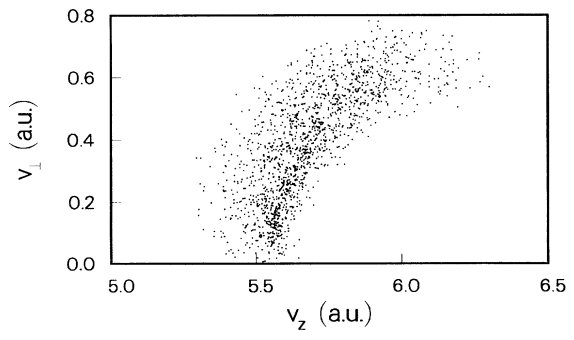

FIG. 2. Velocity distribution of electrons originally bound in a wake-riding state inside the foil after single scattering in a pure Coulomb potential of $\bar{p}$ ($v_p = 6$ a.u.) upon exit from the solid.

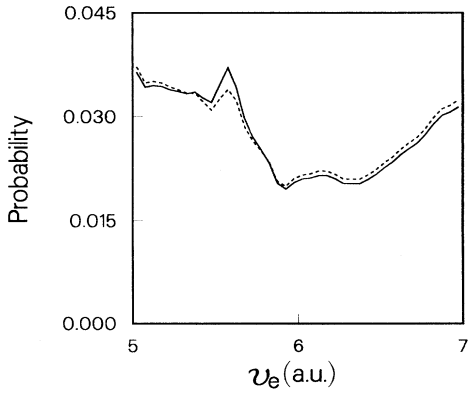

FIG. 3. Normalized convoy electron spectrum for antiprotons ($v_p = 6$ a.u.) emitted into a forward cone of half-angle $\Theta_0 = 5°$ (---) and 2.5° (——).

contribution of slowed-down binary electrons to the customary cusp peaks has also been found to be small.[16]

It should be stressed that the accuracy of the present calculation is limited due to the uncertainty in both the calculation of σ_c and the treatment of the transport of binary electrons. Since the volume of velocity space of the observed spectrum is small compared to the volume of velocity space of all initial conditions for binary electrons which can contribute to the spectrum after multiple scattering, even modest statistical accuracy requires a large number of trajectories. We used a total of 1.8×10^6 initial conditions which resulted in $\simeq 600$ events in the forward spectrum for a cone angle $\Theta = 5°$ and which required smoothing using large bin sizes ($\Delta v \gtrsim 0.40$ a.u.). The validity of the second Born approximation at only moderately high velocities ($v_p \gtrsim 6$ a.u.) may be questionable. Furthermore, we have observed that the cross section depends sensitively on the shape of the wave functions in the exponential tail which, in turn, may be affected by the separable form of the wake-bound state and by the plasmon pole approximation to a free-electron-gas model employed in the present calculation. A more accurate determination of the bound-state spectrum and of the capture cross section is presently underway.[11]

In conclusion, our calculation indicates that forward electron emission by antiprotons propagating through solids may provide the first direct evidence for the existence and formation of wake-bound states in the dynamical polarization potential. A velocity range of $v_p \sim 4$–6 a.u. appears to be optimal for the observation. At lower velocities wake structures become less pronounced and the beam quality deteriorates. At higher velocities the capture cross section into the wake becomes so small compared to the binary electron emission cross section that the peak of wake-riding electrons might be overshadowed by slowed-down binaries.

One of us (J.B.) is indebted to Y. Yamazaki for many stimulating discussions on $\bar{p}$ experiments and to P. Echenique and R. Ritchie for several valuable suggestions. This work is supported by the National Science Foundation and by the U.S. Department of Energy under Contract No. DE AC05-84OR21400 with Martin Marietta Energy Systems, Inc.

[1]L. Andersen, in *Electronic and Atomic Collisions,* edited by H. Gilbody, W. Newell, F. Read, and A. Smith (Elsevier, Amsterdam, 1988), p. 451.

[2]J. McGuire, Phys. Rev. Lett. **49**, 1153 (1982); J. Reading and A. Ford, Phys. Rev. Lett. **58**, 543 (1987).

[3]R. Olson and T. Gay, Phys. Rev. Lett. **61**, 302 (1988).

[4]Y. Yamazaki *et al.*, CERN Report No. CERN-PSCC 87-39 (unpublished), p. 108; CERN Report No. CERN-PSCC 87-40 (unpublished), p. 108.

[5]G. Basbas, Nucl. Instrum. Methods B **4**, 227 (1984), and references therein.

[6]W. Brandt and R. Ritchie, Phys. Lett. **62A**, 374 (1977); M. Day, Phys. Rev. Lett. **44**, 752 (1980).

[7]M. Breinig *et al.*, Phys. Rev. A **25**, 3015 (1982).

[8]F. Drepper and J. Briggs, J. Phys. B **9**, 2063 (1976).

[9]C. Garibotti and J. Miraglia, Phys. Rev. A **21**, 572 (1980); M. Brauner and J. Briggs, J. Phys. B **19**, L325 (1986).

[10]V. Neelavathi, R. Ritchie, and W. Brandt, Phys. Rev. Lett. **33**, 302 (1974); P. M. Echenique, R. Ritchie, and W. Brandt, Phys. Rev. B **20**, 2567 (1979); A. Mazarro, D. Echenique, and R. Ritchie, Phys. Rev. B **27**, 4117 (1983); J. Ashely and P. Echenique, Phys. Rev. B **31**, 4655 (1985); A. Rivacoba and P. Echenique, Phys. Rev. B **36**, 2271 (1987).

[11]J. Müller and J. Burgdörfer (to be published).

[12]J. Briggs and L. Dubè, J. Phys. B **13**, 771 (1980).

[13]Y. Yamazaki and N. Oda, Nucl. Instrum. Methods **194**, 415 (1982); P. Echenique and R. Ritchie, Phys. Lett. **111A**, 310 (1985).

[14]R. Shakeshaft and L. Spruch, Rev. Mod. Phys. **51**, 369 (1979).

[15]J. Burgdörfer (to be published).

[16]H. Schröder, Z. Phys. D **7**, 65 (1987).